AD610257

PERFORMANCE OF LANGMUIR PROBES
IN MEASUREMENTS ABOARD
A REENTRY VEHICLE

SHIMSHON   FRANKENTHAL

American Science and Engineering, Inc.

11 CARLETON STREET
CAMBRIDGE 42, MASSACHUSETTS

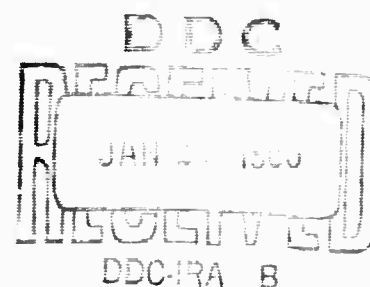CONTRACT NO. AF 19 (628) - 2367

PROJECT NO. 8662

ARPA ORDER 363-62-Amd 2

FINAL REPORT

31 JANUARY 1964

DDC
RECEIVED
JAN 1963
DDC-IRA B

PREPARED FOR

AIR FORCE CAMBRIDGE RESEARCH LABORATORIES
OFFICE OF AEROSPACE RESEARCH
UNITED STATES AIR FORCE
BEDFORD, MASSACHUSETTS

BLANK PAGE

AFCRL-64-975

ASE-510

PERFORMANCE OF LANGMUIR PROBES

IN MEASUREMENTS ABOARD

A REENTRY VEHICLE

Shimshon Frankenthal

American Science and Engineering, Inc.
11 Carleton Street
Cambridge 42, Massachusetts

FINAL REPORT

Contract AF 19 (628)-2367

Project No. 8662
ARPA Order 363-62 -Amd 2

31 January 1964

FOREWORD

The work reported here pertains to the interpretation of data from Langmuir probes flown aboard a reentry vehicle. The problem is unusual because of the peculiar environmental conditions, and because the quantity of data actually telemetered is severely limited. It is, therefore, clear that proper interpretation of the data requires a thorough study of the various methods of analyzing probe characteristics, and in particular of the restriction imposed between the two factors mentioned above on the applicability and reliability of these methods. This study constitutes the major part of this report. The emphasis in the research program was directed under the guidance of the Air Force scientific monitor.

The author wishes to take this opportunity to gratefully acknowledge the help extended him by Drs. J. W. Carpenter and O. P. Manley and Mr. Y. M. Treve of AS&E.

ABSTRACT

The theory of Langmuir probes is reviewed. Particular attention is accorded to the interpretation of data obtained when the probe is in saturation, and to plasmas in which the characteristic ion and electron energies are comparable. Various methods for interpreting the probe measurements are enumerated.

This information is employed in the subsequent discussion, which concerns the performance of Langmuir probes flown aboard a re-entry vehicle, and the interpretation of data telemetered from these probes.

TABLE OF CONTENTS

LIST OF ILLUSTRATIONS

I. INTRODUCTION

1.1 Objective

The objective of this report is to evaluate the performance of Langmuir probes, flown aboard a re-entry vehicle in an extensive experiment whose aim was to gain information regarding some of the electrical properties (ion and electron temperatures and densities) of the medium surrounding the vehicle.

Other instruments flown aboard the vehicle measured other electrical properties. The data obtained from these instruments might be employed to check, supplement, or even improve the results of the probe observations. However, we have restricted our attention to the probe itself, and to the evaluation of its capability as an independent, isolated instrument.

1.2 Organization

This report begins with a general review of the present status of probe theory, delving in some detail into some of the controversial aspects of the theory. This material is subsequently employed in the discussion of the re-entry vehicle experiments.

II. PROBE THEORY -- THE ELECTRON RETARDATION REGION

2.1 General Features of Langmuir Probe Curves

A Langmuir probe is a small conductor imbedded in a plasma. By varying the potential of the probe (and we need not, at the moment, be concerned with the manner in which this is accomplished) and measuring the current it delivers to, or draws from, the plasma, we determine the V-I characteristic of the plasma. From this so-called probe curve we can, in principle, expect to infer information regarding the densities of ions and electrons in the plasma and their distribution in energy.

The general features of the voltage-current characteristic of a probe immersed in a plasma are shown in Figure 2.1 (Reference 1). When the probe delivers no current, it floats to a potential V_f which is generally negative with respect to the plasma. The reason is that the initial rate of arrival of electrons usually far exceeds that of the ions, so that a negative charge develops on the probe. This charge gives rise to a voltage which repels the slower electrons, hence reduces their rate of arrival. The process continues until the rate of arrival of electrons is reduced to that of the ions.

If the potential is decreased below V_f, more electrons are repelled, amounting to a negative current from the probe to the plasma. The ion saturation regime is reached when all electrons are repelled.

If, on the other hand, the probe potential is increased above V_f, more electrons are allowed to reach the probe, giving rise to a positive current from the probe to the plasma. Eventually the probe reaches the plasma potential, at which neither ions nor electrons experience any force on their way to the probe (in Figure 2.1, this potential was chosen as the reference potential). When the probe potential exceeds the plasma potential, ions are repelled from the probe. The electron saturation regime is reached when all ions are repelled.

2

V-I CHARACTERISTIC OF LANGMUIR PROBE

ELECTRON
RETARDATION

ELECTRON SATURATION

V_f

ION SATURATION
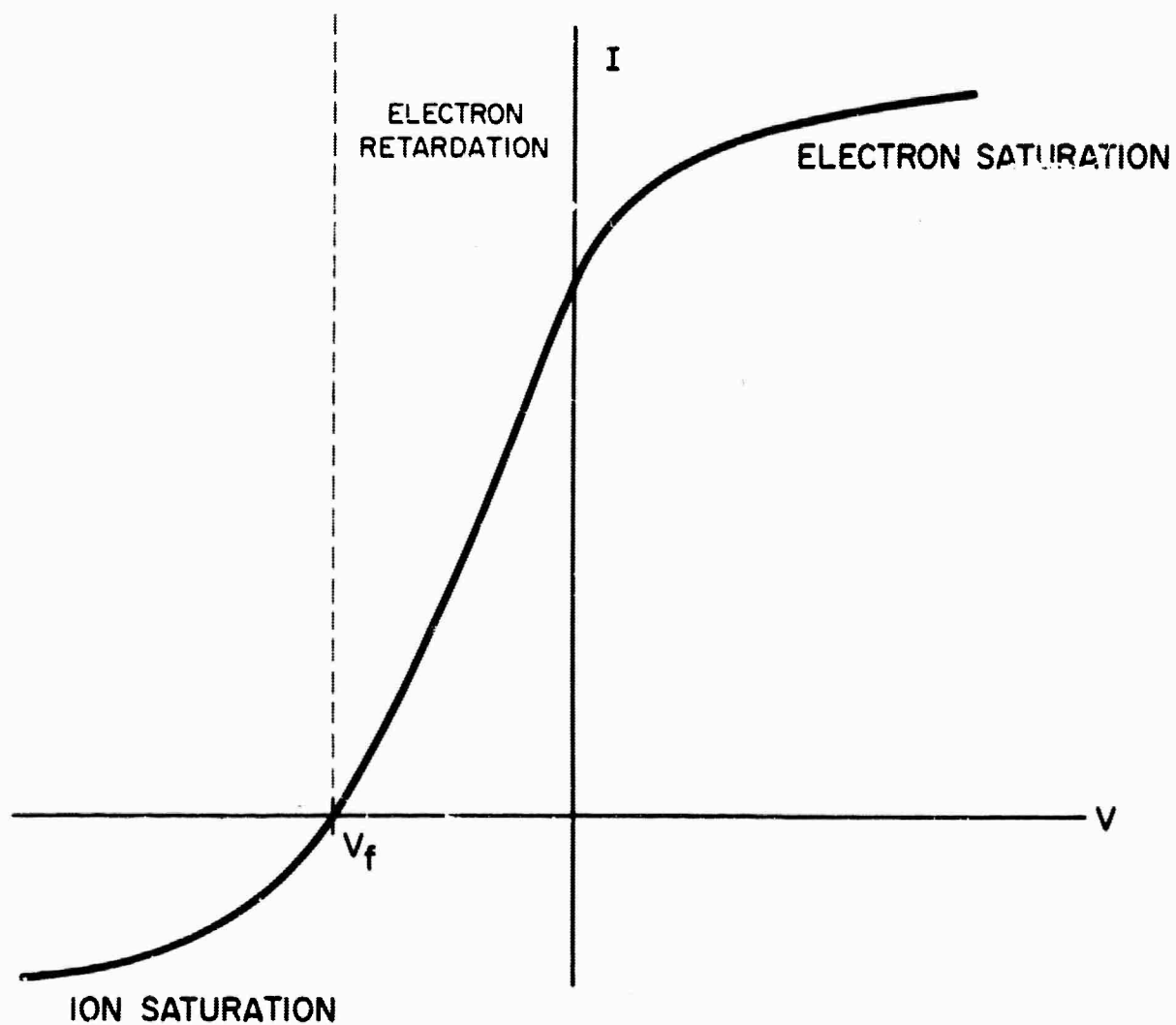
VOLTAGE MEASURED WITH
RESPECT TO PLASMA POTENTIAL

Figure 2.1

3

2.2 Interpretation of the Probe Curve

The interpretation of the probe curve requires that we be able to relate the probe current and voltage to the properties of the undisturbed plasma under observation. In order to accomplish this, it is necessary to describe the motions of particles reaching the probe in terms of the potential in the region surrounding the probe. In order to clarify some of the problems which are inherent to this process, it is helpful to express the probe current in component form, as follows:

$$I = I_{-r} + I_{+a} \qquad \text{for} \qquad V < 0 \quad \text{(a)}$$

$$(2.2.1)$$

$$I = I_{-a} + I_{+r} \qquad \text{for} \qquad V > 0 \quad \text{(b)}$$

where V is the potential of the probe with respect to the plasma, I the current, the subscripts $+$ and $-$ identify the ion and electron components of the current, respectively, and the subscripts a and r indicate whether the particles contributing to the current are accelerated or retarded in their motion toward the probe.

Loosely speaking, it may be stated that the mathematical description of the behavior of particles in retarding potential is considerably more tractable than that of particles in accelerating potentials, in that geometrical considerations affect the latter much more than the former. An illustration of this statement appears in Section 3.2. As we shall see shortly, this distinction between accelerated and retarded particles is almost inextricably related to the distinction between the regimes of saturation and the intervening regime, which we shall call the electron retardation region. We also observe, in passing, that from an experimental point of view, secondary phenomena (such as probe surface bombardment) are considerably more significant when the particles whose behavior dominates a given situation are in extreme acceleration.

4

2.3   The Electron Retardation Region

In accordance with what was said above, there appears to be general agreement as to the probe phenomena related to the region between the plasma potential and the floating potential. In this region, we are concerned with Equation 2.2.1a. Although this equation contains the term I_{+a}, representing the (accelerated) ion component of the current, this term is overshadowed, over most of the region in question, by the electron component.

The probe characteristic in this region can be made to yield considerable information. By twice differentiating the current with respect to the voltage, one obtains the distribution function of the electrons (Druyvestein, Reference 2) provided it is isotropic and the probe surface is convex. Furthermore, in the rather common case where the electron distribution is Maxwellian, the well-known exponential relationship obtains between the probe current and voltage. (Reference 1)

$$ I \propto \exp \left(- \frac{qV}{kT_-} \right) \qquad (2.3.1) $$

where q is the electronic charge and T_- the electron temperature. This renders the identification of a Maxwellian distribution, and the determination of its temperature, relatively easy.

Finally, by way of introduction to the problem of saturation, one might cite an additional fact which simplifies the interpretation of probe data in the electron retardation region, namely, the relative insignificance of space charge sheath effects in this region. This is true in particular in the vicinity of the plasma potential. Therefore, in the determination of the current density (which is, after all, the quantity provided by the kinetic theory arguments) from the probe current

$$ i = \frac{I}{A} \qquad (2.3.2) $$

there is no question as to the area A which should be used - it is the surface area of the probe. As we shall see shortly, this is not the case in the saturation regime.

III.   PROBE THEORY - SATURATION

3.1   Saturation Phenomena and Sheaths

The electron retardation region of the probe characteristic provides information regarding the distribution of the electrons, and, in particular, yields their temperature in the Maxwellian case. The saturation regime provides information regarding the particle densities.

By contrast to what was said above regarding the electron retardation regime, the interpretation of data pertaining to the saturation regime is relatively difficult and, at the moment, quite controversial. In this regime the probes are heavily sheathed with space charge since the density of one of the species completely dominates that of the other near the probe. The interpretation of the probe data therefore requires an analysis of the sheath which represents a sharp transition from the plasma to the probe.

The analysis of a sheath requires a solution of Poisson's equation

$$\nabla^2 \phi (\vec{r}) = - \frac{1}{\epsilon_o} \rho (\phi, \vec{r}) \qquad (3.1.1)$$

where ϵ_o is the permittivity of free space, $\phi(\vec{r})$ is the potential at the point $\vec{r}$, and where the charge density

$$\rho (\phi, \vec{r}) = |q| [n_+ (\phi, \vec{r}) - n_- (\phi, \vec{r})] \qquad (3.1.2)$$

represents the difference between the densities n_+ and n_- of positive and negative particles. These densities are given by

$$n_\pm (\phi, \vec{r}) = \int d^3 \vec{v} f_\pm (\vec{v}, \vec{r}) \qquad (3.1.3)$$

where $f_\pm$ is the distribution function and $\vec{v}$ the velocity. (In infinite planar geometries, the position argument $\vec{r}$ on the right hand side of Equation 3.1.1

6

is absent, simplifying matters considerably). The discussion in the following section will illustrate the difficulties involved in this approach and the differences between retardation and acceleration mentioned above, and will introduce pertinent results for subsequent use in this report.

3.2 The Ion Saturation Region - Approximate Analysis

Early attempts to treat the problem of saturation sought to avoid the problem of solving Poisson's equation in full by subdividing the region ahead of the saturated probe into three major regimes, each of which could then be treated by a simplified approach (see Figure 3.1 and References 3 through 7). These regimes are: (1) The body of the plasma, which is neutral and unperturbed by the presence of the probe; (2) The pre-sheath, which is quasi-neutral, in that

$$ n_+ - n_- \ll n_+ \text{ or } n_- \qquad (3.2.1) $$

and yet is permeated by weak fields. The cumulative effect of these weak fields is nevertheless significant since a cold ion emanating from the body of the plasma will be accelerated to one-half the electron temperature in its passage through the sheath; and (3) The space charge sheath, in which space charge phenomena are significant because it is populated primarily by particles of one species.

In solving the problem, one first determines the variation of the potential $\phi_{qn}(\vec{r})$ in the pre-sheath by equating n_+ to n_-, by virtue of the quasi-neutral assumption. One next determines the transition surface between the pre-sheath and the space-charge sheath as the point $\vec{r}_s$ where $\nabla \phi_{qn}$ becomes infinite, since here clearly the quasi-neutral assumption breaks down. Finally, one treats the space-charge sheath as a one-particle sheath, to which the well known three halves power law applies (References 3 and 10).

7

SPACE CHARGE SHEATH QUASI-NEUTRAL PRE-SHEATH NEUTRAL BODY OF THE PLASMA

PROBE

THE "3/2 POWER" POTENTIAL SOLUTION

THE QUASI-NEUTRAL POTENTIAL SOLUTION $\phi_{qn}(\bar{r})$

SMOOTHED REGION

r_p r_s r_l r
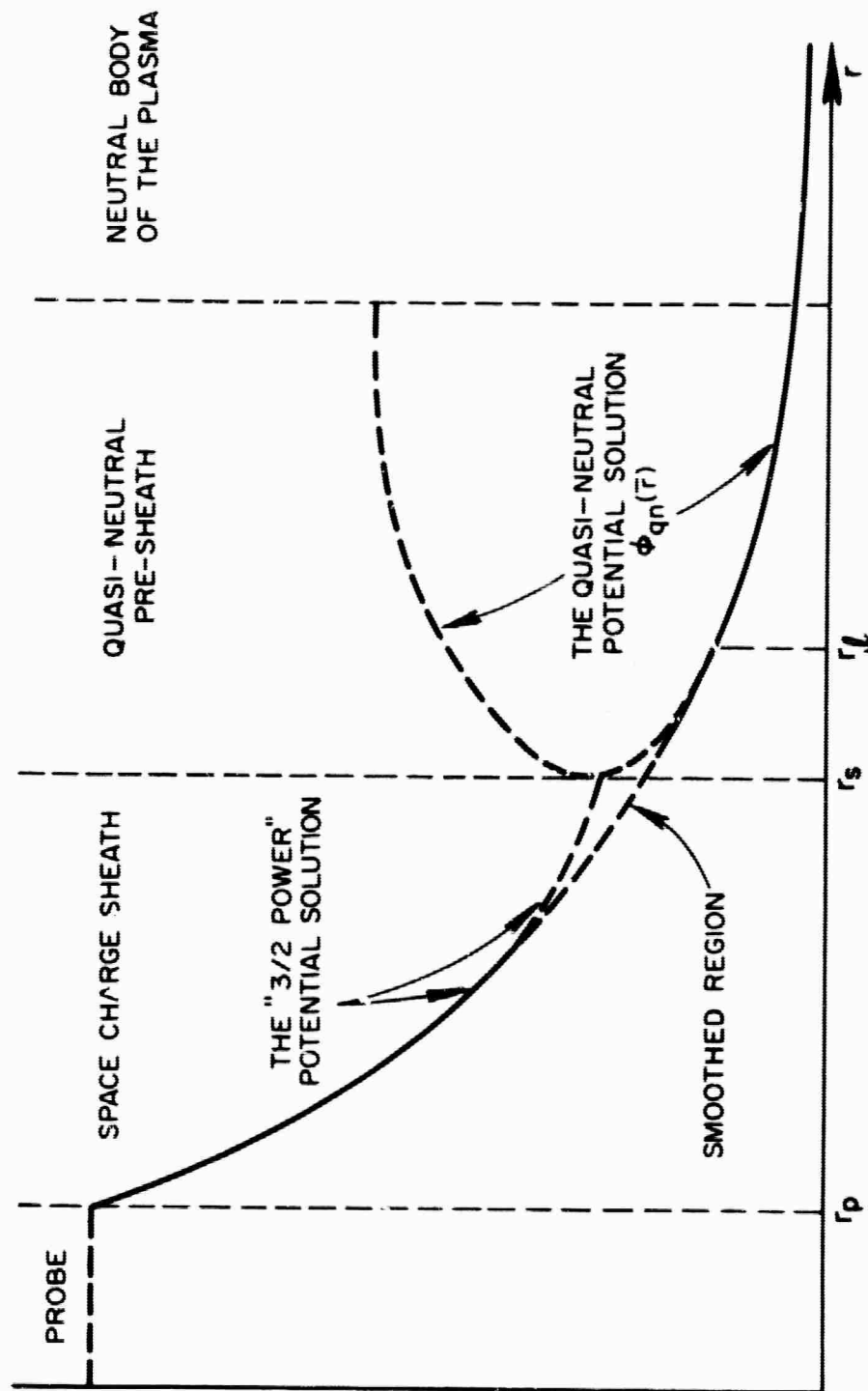
THE TRANSITION BETWEEN A PLASMA AND A SATURATED PROBE

Figure 3.1

8

No problems arise when this approach is applied to a planar case (References 3 and 4). However, in applying it to the spherical geometry, Bohm, Burhop and Massey (Reference 5, later called B. B. M. in this text) found what came to be called "limitation motion" (Reference 7). Briefly, the radial motion of a particle in a spherical geometry is governed, via the energy conservation equation

$$\frac{1}{2} m v_r^2 + \psi = E = \text{constant} \tag{3.2.2}$$

by the effective potential

$$\psi = q \phi + \frac{J^2}{2mr^2} \tag{3.2.3}$$

which accounts for the angular motion via the angular momentum J. Here E is the total energy of the particle. Recalling the distinction between retarded and accelerated particles (cf. Section 2.2) note that, when the electrical potential ϕ is retarding, $(q\phi > 0)$ both components of ψ are positive and decrease monotonically with r. Thus, if a particle is to reach a given radial position r, its energy must satisfy the clear-cut requirement

$$E \geq \psi(r, J) \tag{3.2.4}$$

On the other hand, for accelerating potentials, $q\phi$ is negative. Under these conditions, a local maximum may develop in the effective potential (see Figure 3.2) at some position r_m. Therefore, the energy of a particle which can reach a radial position $r < r_m$ must satisfy the requirement

$$E \geq \max \left[\psi(r, J), \psi(r_m, J) \right] \tag{3.2.5}$$

where max (A, B) implies the larger of the two quantities A and B.

9

TYPICAL PLOT OF THE EFFECTIVE POTENTIAL ψ
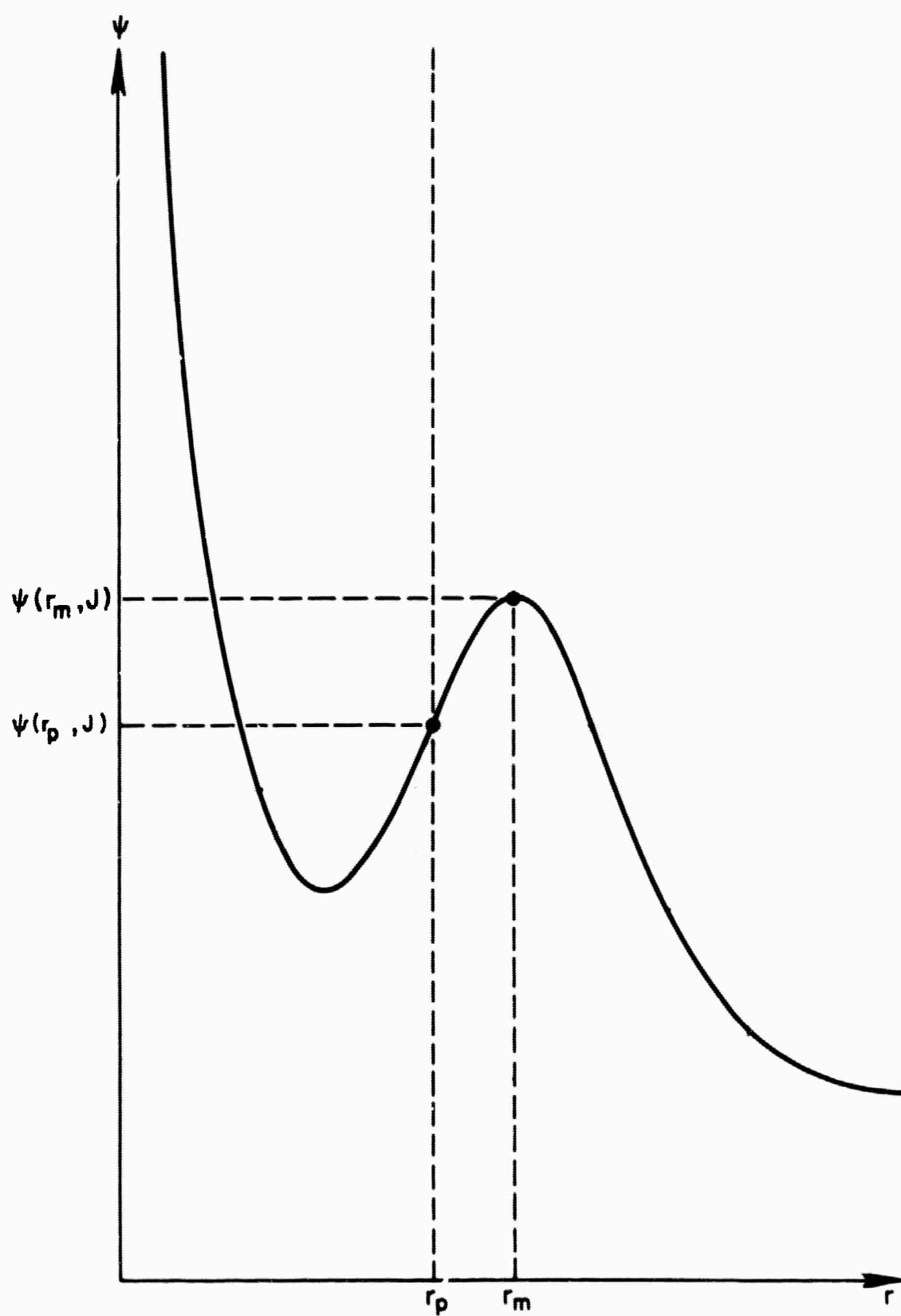
Figure 3. 2

It is obvious that this complicates the formulation of the kinetic-theory integral for n_+ (for ion sheaths). However, of more immediate physical interest is the fact that, if the ion distribution is assumed to be monoenergetic, there exists as a result of this phenomenon a well defined "limitation sphere" of radius r_l, which replaces the probe as an effective collector because any particle that crosses this sphere is bound to reach the probe. The remainder of the analysis is then concerned with the relation between this radius and the sheath radius r_s.

The analysis of B.B.M. leads to the following expression

$$I \sim I_{+s} = cn_o q \sqrt{\frac{2kT_-}{m_+}} A_s \qquad (3.2.6)$$

where

$\qquad I_{+s}$ is the ion saturation current,

$\qquad m_+$ is the ionic mass,

$\qquad T_-$ is the electron temperature,

$\qquad A_s$ is the sheath area, and

$\qquad n_o$ is the ion (or electron) density deep in the plasma.

The factor c lumps in corrections which account for the ratio

$$\beta = \frac{T_+}{T_-} \qquad (3.2.7)$$

of ion to electron temperature and the ratio of the sheath radius to the limitation radius. This factor c is about 0.4, and varies by 20% for $o < \beta < 0.5$.

11

The conclusions of the B. B. M. analysis are: (1) that ion collection by the probe is not significantly affected by the ion temperature; and (2) that the probe current I_{+s} to be used in Equation (3.2.6) for the purpose of determining n_o (with T_- known) should be the value obtained by extrapolating the saturation portion of the probe curve to the plasma potential, i.e. to the point where there is no sheath and A_s may be replaced by the surface area of the probe, A_p, unambiguously.

The requirement that the use of Equation (3.2.6) be restricted to the plasma potential current stems from two reasons: (a) the saturation current density

$$j_{+s} = \frac{I_{+s}}{A_s}$$

computed by B. B. M. may be incorrect because it does not account for secondary phenomena, such as secondary emission which arises when the probe potential is large and the ions are highly accelerated; and (b) because B. B. M. did not chose to employ the three-halves power law which relates the sheath and probe radii r_s and r_p to the probe voltage and the current density, and thus accounts for the growth of the sheath with probe voltage. Thus, if we disregard the effect of secondary emission, we can achieve some degree of generalization of these results by employing the generalized form of the three-halves power law, whicn obtains across the single-particle space charge sheath, namely,

$$I = \frac{4\sqrt{2}}{9} \sqrt{\frac{q}{m_+}} \frac{V^{3/2}}{\left[\gamma\left(\frac{r_s}{r_p}\right)\right]^2} \qquad (3.2.8)$$

In this form, $\gamma\left(\frac{r_s}{r_p}\right)$ is a non-dimensional function, tabulated by Langmuir and Blodgett (References 10 and 11), which accounts for the growth of the spherical sheath at any probe potential. The need to extrapolate to plasma potential is thus circumvented.

A correction to this method has recently been proposed by Kagan and Perel (References 6 and 7, later called K. P. in this text). They note that it is not correct to treat the space charge sheath as dominated by a single particle

12

species throughout, since a considerable number of electrons are still present on the plasma side of this sheath. They therefore propose the subdivision of the space charge region into an ion region and a reflection region in which electrons are being turned back toward the plasma (see Figure 3.3). The demarcation line is the point r_ρ at which the space charge density is maximal. Strictly speaking, Equation (3.2.6) applies to the ion region, so r_s must be replaced by r_ρ in that equation. It is therefore necessary to replace the quantity A_s in Equation (3.2.6) by A_ρ, the outer surface area of the ion sheath, which requires the use of an accomodation factor α (β) instead of c in Equation (3.2.6). This accomodation factor accounts for the effect of the reflection region, and, for a given β, must lie in the range indicated in Figure 3.4. The range is fairly wide for low values of β, but narrows down considerably as β increases. The argument presented by the authors indicates that, for high probe potentials, the value of α should be chosen close to the upper limit. The argument is born out by the fact that the K.P. computed results agree well with the results of an exact approach to the problem, to be discussed presently, whereas the equations and accomodation factors proposed by B.B.M. differ by a factor of 2. (References 6 and 7).

The use of Equations (3.2.6) and (3.2.8), in either the K.P. version or the modified B.B.M. version, would permit the determination of the ion density n_o, given the electron temperature T_- and a point (V, I) on the saturation portion of the curve, by the following procedure:

(1) From Equation (3.2.8), determine the value of the factor
$$\gamma\left(\frac{r_s}{r_p}\right);$$

(2) Employing the Langmuir and Blodgett tabulation, determine $\dfrac{r_\rho}{r_p}$ (or $\dfrac{r_s}{r_p}$ as the case may be), hence r_ρ (or r_s); and,

(3) Using (3.2.6) and the equation
$$A_s = 4\pi r_s^2 \quad \text{or} \quad A_\rho = 4\pi r_\rho^2 \qquad (3.2.9)$$
determine n_o.

13

PROFILES OF THE POTENTIAL, ION DENSITY, ELECTRON DENSITY AND CHARGE DENSITY ACROSS THE SHEATH
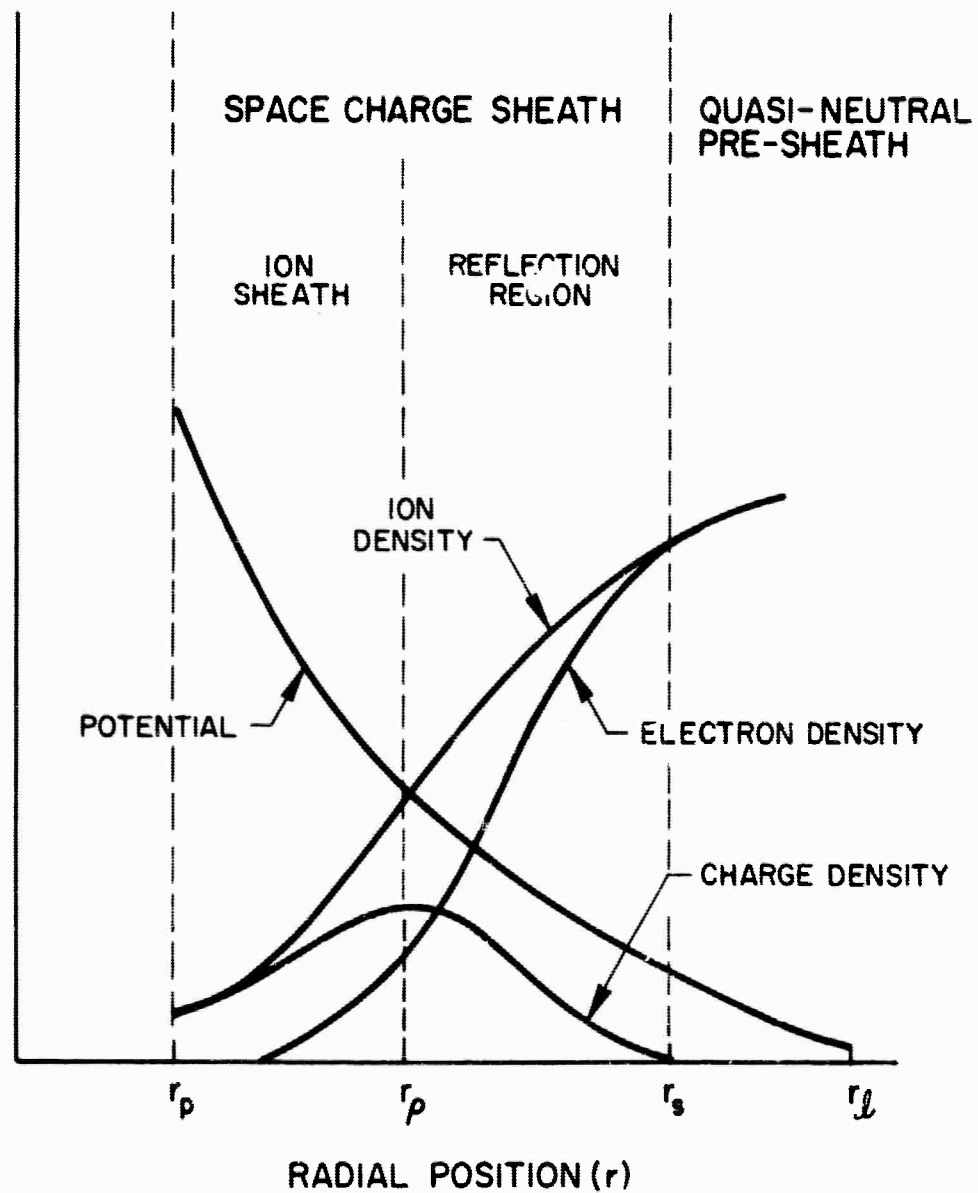
REF: AFTER KAGAN AND PEREL[7]

Figure 3.3

14

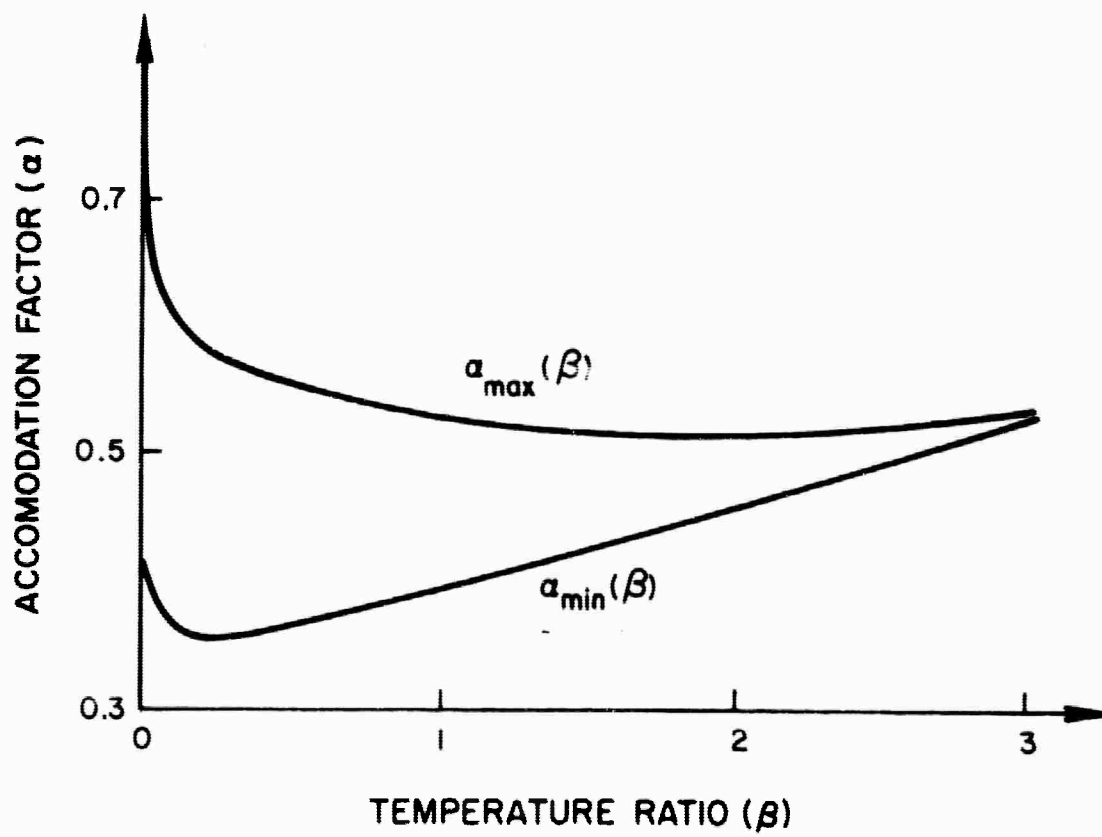# THE ACCOMODATION FACTOR a

REF: AFTER KAGAN AND PEREL[7]

Figure 3. 4

The procedure is rather simple, an advantage which is, however,
c et by a measure of uncertain'y (a factor of 2 at most) in the choice of
accommodation factors. It might be pointed out that the need to use such
factors is inherent in the approximations used in this method, namely, the
artificially sharp subdivision of the plasma-probe transition into distinct
regimes.

3.3   Ion Saturation - Exact Solution

A.1 alternative method for interpreting ion saturation measurements is
provided by the use of the results of an exact solution of the same problem,
proposed by Bernstein and Rabinowitz (Reference 8, later called B.R. in
this text).* They followed the self-consistent approach, outlined at the end
of Section 3.1, without resorting to the subdivision of space into various
regimes, and solved Poisson's equation for the full, continuous transition
from probe to plasma. The results of this solution are presented graphically
as plots of the non-dimensional potential

$$= - \frac{q\phi}{kT_-} \tag{3.3.1}$$

versus the non-dimensional radius   -

$$= \frac{r}{\lambda_d} \tag{3.3.2}$$

where

$$\lambda_d = \sqrt{\frac{\epsilon_0 kT_-}{n_0 q^2}} \tag{3.3.3}$$

is the Debye length. The non-dimensional probe current

* A limited form of their results, applicable to the case where the plasma
ions are cold ($\beta = o$), was earlier given by Allen, Boyd and Reynolds
(Reference 9).

16

$$\iota = \frac{|q|}{kT_-} \left(\frac{m_+}{2kT_-}\right)^{1/2} \frac{1}{\epsilon_0 \pi} I \qquad (3.3.4)$$

and the temperature ratio β are used as parameters. Typical plots for $o < \beta < 0.1$ are given in Reference 8. The profiles for $\beta = 1$ are presented in Figures 3.5a and b.

These results can be reprocessed graphically (by picking of the X and ι intercepts of a vertical line $\xi = \xi_p$ in Figure 3.5) to produce non-dimensional characteristic curves for probes of various radii, such as are shown in Figures 3.6a and b for the case $\beta = 1$, where χ_p is the non-dimensional probe voltage and ξ_p is the non-dimensional probe radius.

Although exact, the graphical results obtained by this method are cumbersome to use. In order to extract the ion density and temperature, it is necessary to have two points (V, I) on the ion saturation portion of the curve. With the electron temperature, T_-, known, the procedure is as follows:

(1) From V, I, and T_-, determine χ_p and ι (Equations 3.3.1 and 3.3.4);

(2) Locate the point (χ_p, ι) on each family of probe curves corresponding to a given β (such as are shown in Figure 3.6), and determine ξ_p;

(3) Construct the locus (β, ξ_p) corresponding to the point $(\chi_p, \iota$); and,

(4) Repeat the above steps for the second point (V, I).

(5) The intersection of the two loci (β, ξ_p) yields the values of β and ξ_p. From these, the ion energy is determined as (cf. Equation 3.2.5))

$$T_+ = \beta T_- \qquad (3.3.5)$$

and the density is determined using the known probe radius, r_p, and Equations (3.3.2) and (3.3.3)

$$n_0 = \frac{\epsilon_0 kT_-}{q^2} \frac{\xi_p^2}{r_p^2} \qquad (3.3.6)$$
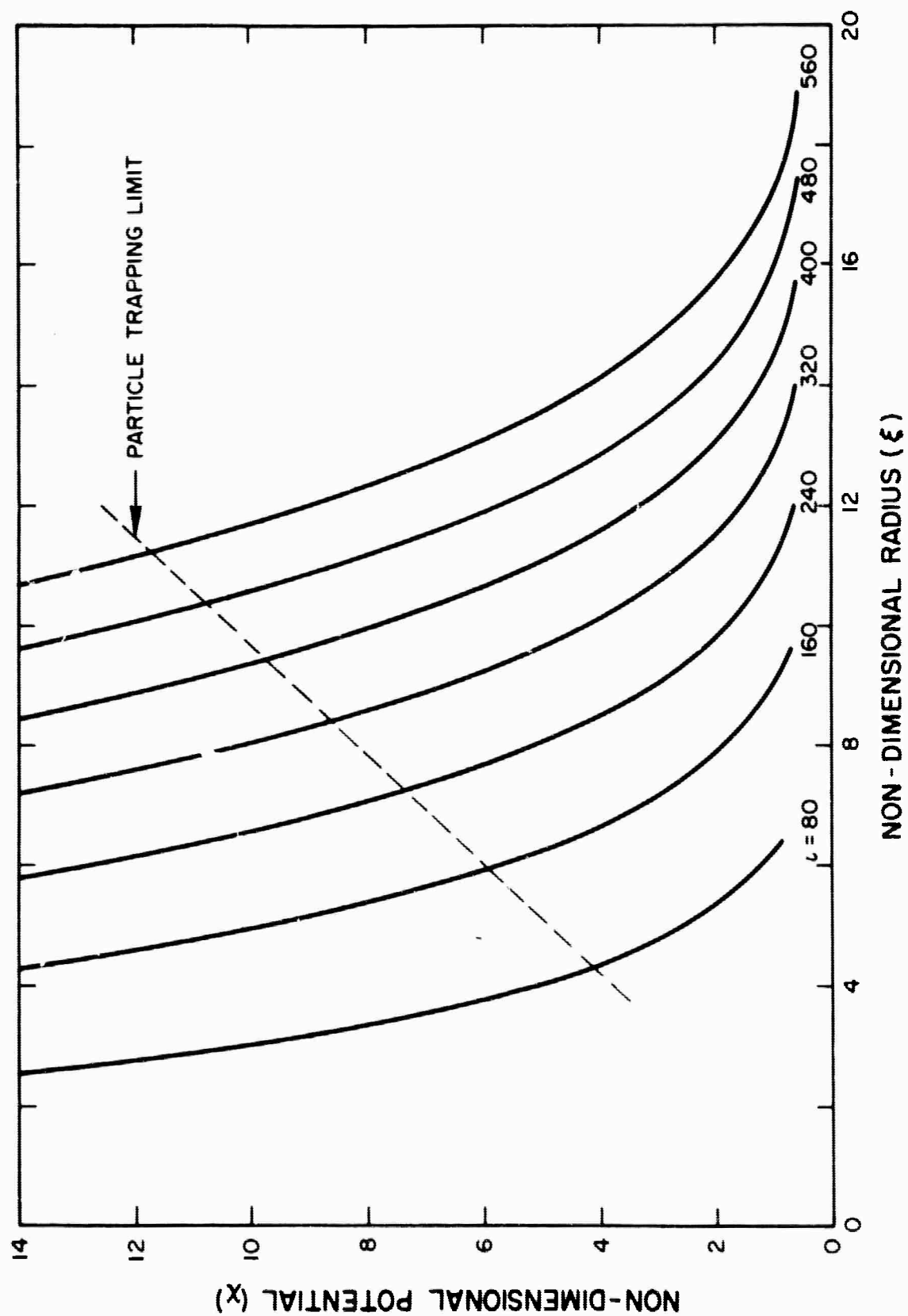
17

POTENTIAL PROFILES FOR VARIOUS PROBE CURRENTS

(β = 1.0)

Figure 3.5a

18

POTENTIAL PROFILES FOR VARIOUS PROBE CURRENTS
($\beta = 1.0$; PARTICLE TRAPPING IGNORED)

Figure 3.5b

19

PROBE CURVES FOR VARIOUS PROBE RADII

($\beta = 1.0$)

Figure 3.6a

PROBE CURVES FOR VARIOUS PROBE RADII

($\beta = 1.0$; PARTICLE TRAPPING IGNORED)

Figure 3.6b

21

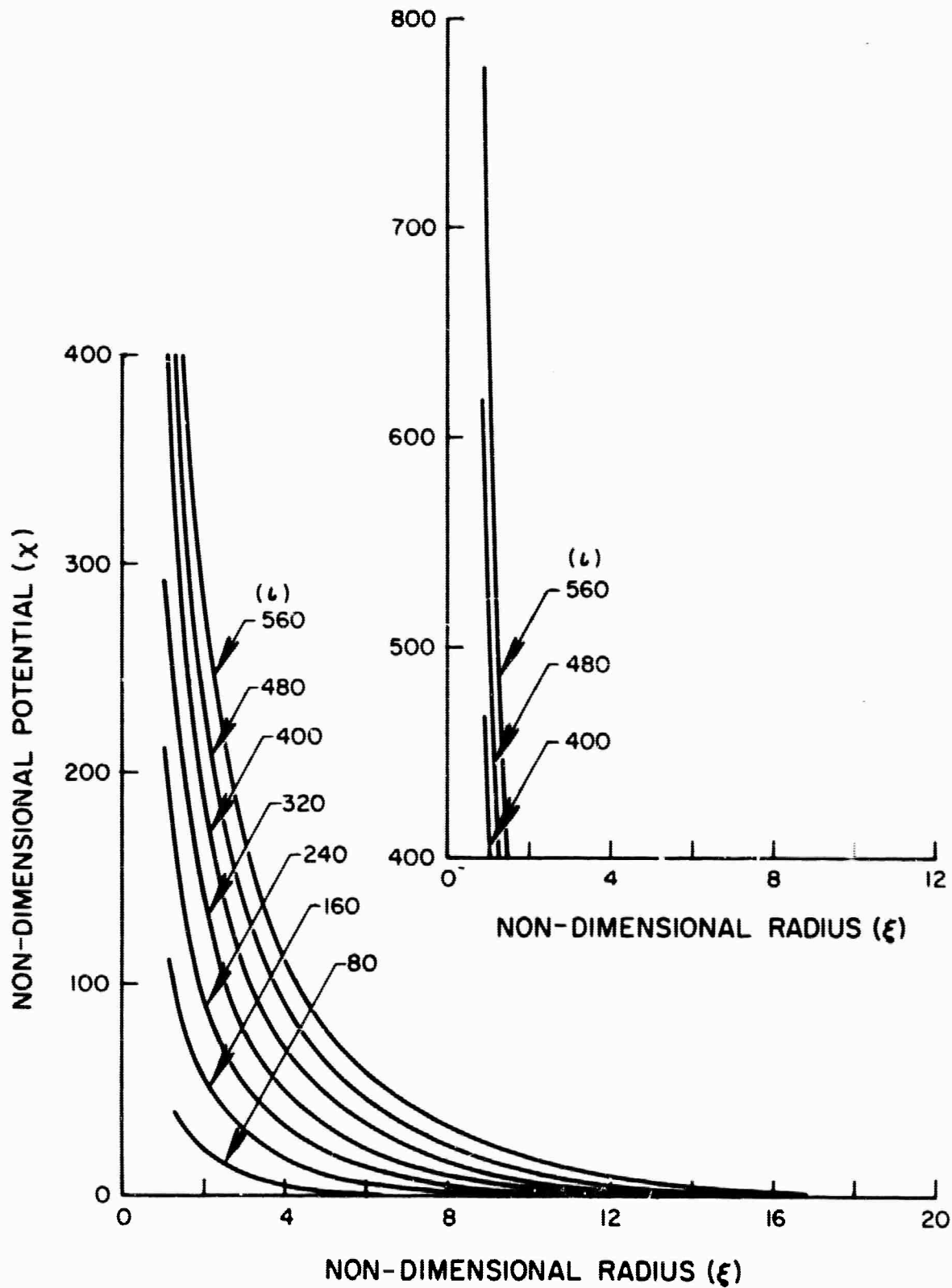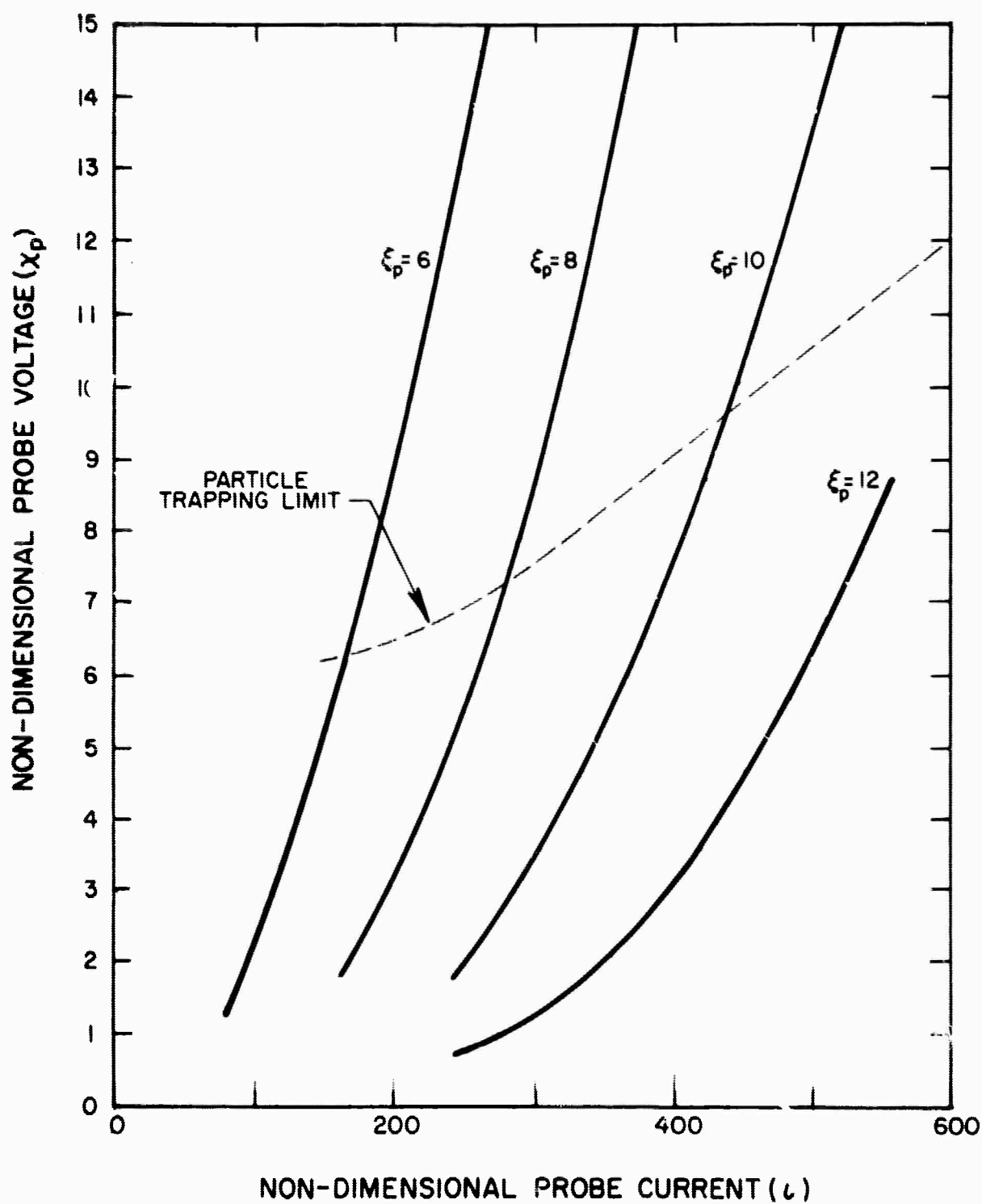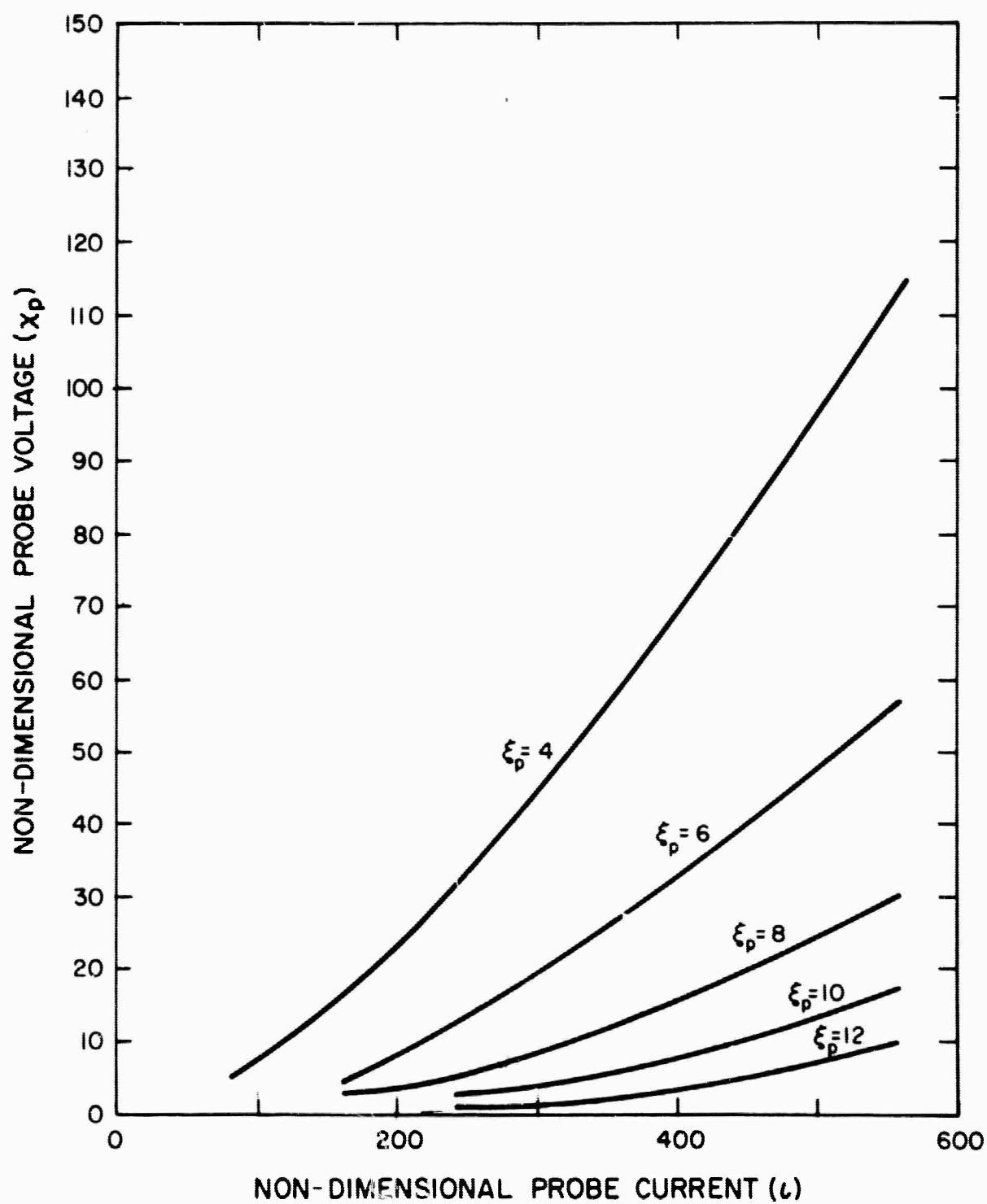The construction in Step (3) above can clearly be prepared in advance, in the form of a sequence of graphs yielding β versus ξ_p with χ_p and ι serving as parameters.

Note, however, that ion current is indeed not too sensitive to the ion energy (it varies only by 20% over the range $0 < \beta < 1$). In fact, corresponding potential profiles (Figure 3.7) and probe curves (Figure 3.8) appear to crowd together increasingly as β is increased, and it may be expected that the curves for $\beta > 1$ are all nearly indistinguishable.

This would prevent the determination of the ion temperature, yet simplify the determination of the density n_o, using a single point (V, I) on the saturation curve (perform Step 1 above, then use Equation (3.3.6)).

The B.R. approach retains most of the physical features of the B.B.M. approach. In particular, the limitation radius plays a prominent role. However, the B.R. treatment reveals an additional feature which has apparently been overlooked by other researchers. Associated with the maxima which develop in the effective potential ψ (cf. Equations 3.2.2, 3 and Figure 3.2) are "wells" of effective potential, lying on the probe side of the maxima. If the probe is sufficiently small, these wells can trap particles. The population of trapped particles is determined by collisions, however rare, and cannot be accounted for in any simple manner. However, they can cause significant changes in the local potential, interact with the maxima, and significantly affect the current reaching the probe.

The possibility of trapping has been ignored in the computations of the high-voltage portions in Figures 3.5 a and b and 3.6 a and b. However, the limit beyond which trapping may occur is clearly indicated. The dependence of this limit on ι and β is shown in Figure 3.9. The problem may be strictly academic, since at the high voltage and secondary phenomena may alter the situation altogether.

It appears, then, that under the conditions assumed in the models considered above, namely

VARIATION OF A TYPICAL POTENTIAL PROFILE
WITH TEMPERATURE RATIO

$(\iota = 320)$

REF: AFTER BERNSTEIN AND RABINOWITZ[8], WITH EXCEPTION
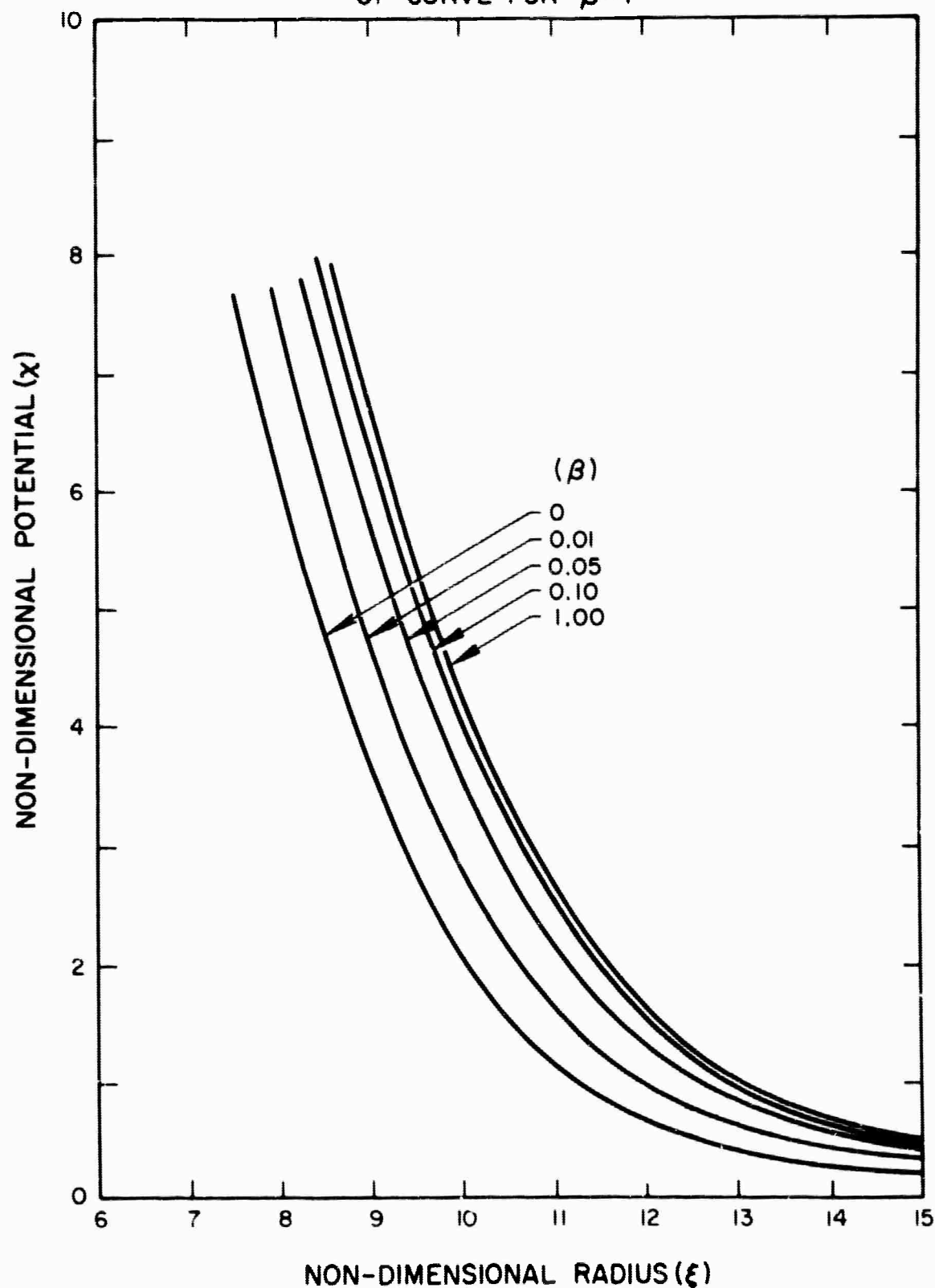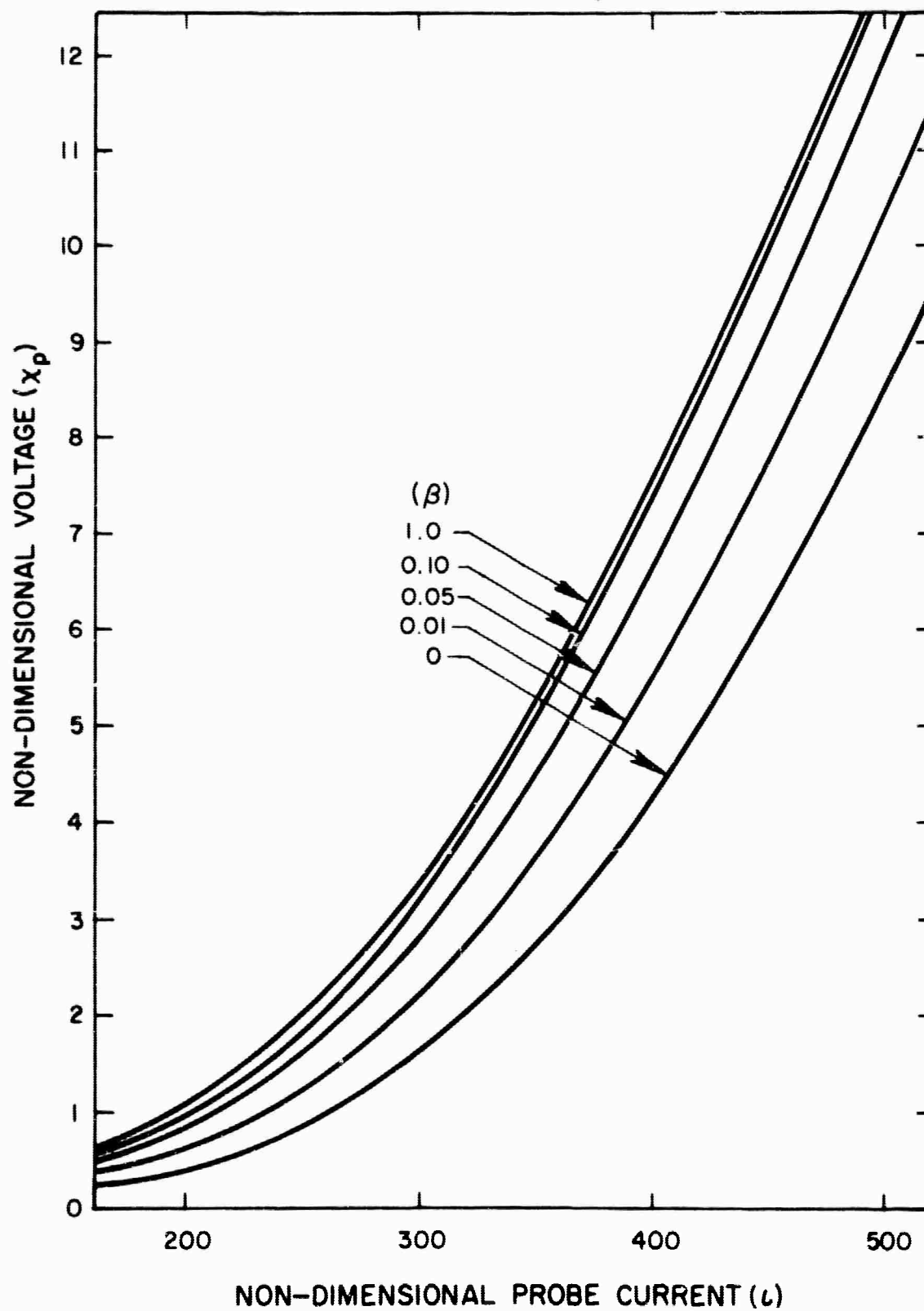OF CURVE FOR $\beta = 1$

Figure 3.7

23

VARIATION OF A TYPICAL PROBE CURVE WITH TEMPERATURE RATIO

($\xi = 10$)

REF.: AFTER BERNSTEIN AND RABINOWITZ [8], WITH EXCEPTION OF CURVE FOR $\beta = 1$

24

Figure 3. 8

DEPENDENCE OF THE TRAPPING RADIUS ON PROBE CURRENT AND TEMPERATURE RATIO

REF: AFTER BERNSTEIN AND RABINOWITZ[8], WITH EXCEPTION OF CURVE FOR $\beta = 1$

Figure 3.9

25
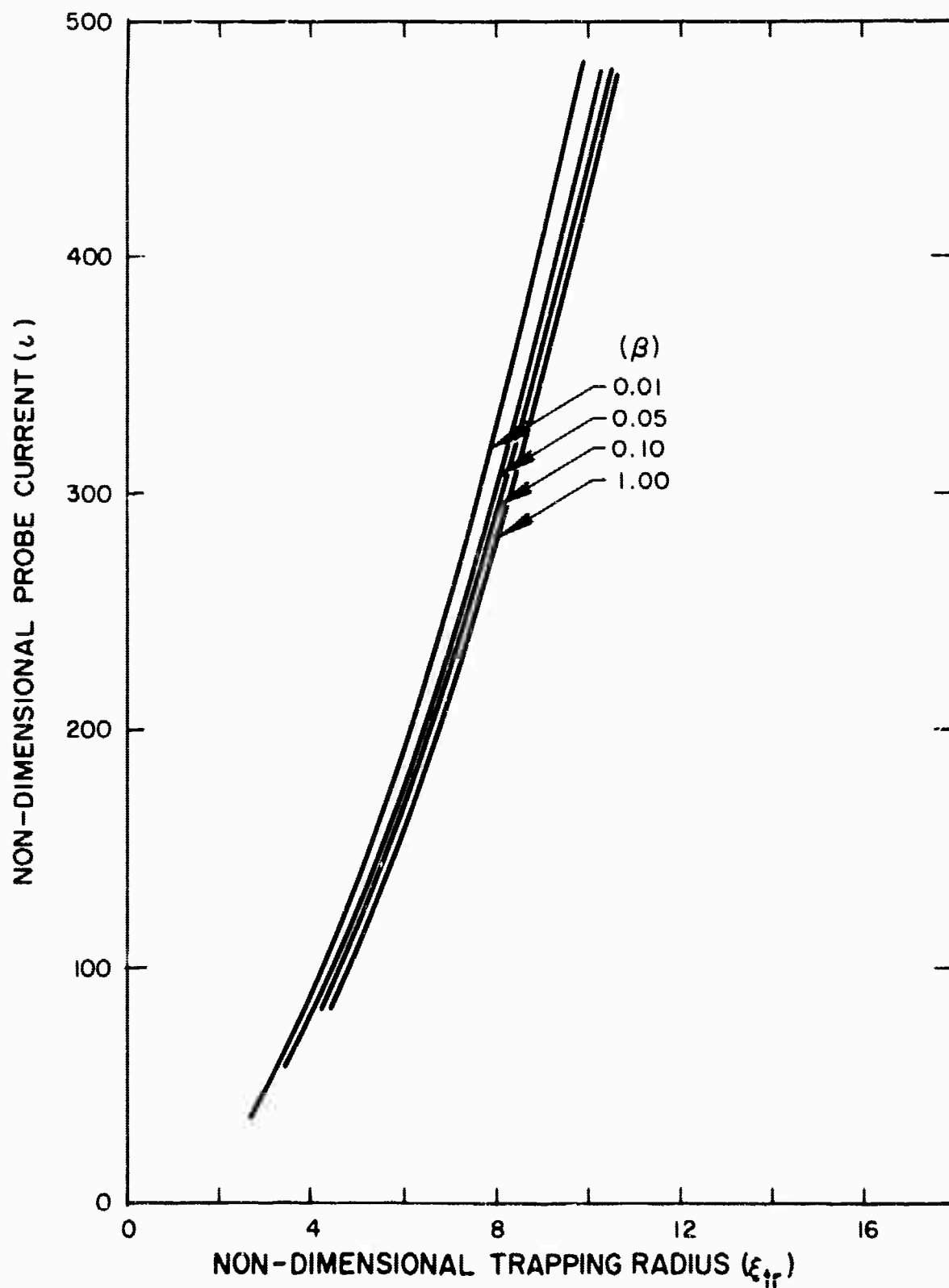
(a) infinite, collisionless plasma,

(b) isotropic ion velocity-distribution, and

(c) finite probe,

true saturation is never reached: the effective collecting area, and with it the probe current, continue to grow with probe voltage. This conclusion must be modified if one of these assumptions is violated, e.g. if the plasma is confined, or if the characteristic dimension of the sheath becomes comparable to the mean free path. However, the manner of interpreting the probe data in either case is not clear at the present. Furthermore, even when the above conditions are satisfied, one should bear in mind the possibility of particle-trapping, which occurs when the probe dimensions are not sufficiently large as compared to the Debye length, or alternatively when the probe voltage is too high (see Figure 3.5).

3.4 The Electron Saturation Regime

The above considerations could be applied, in reverse, to the electron saturation regime. However, to quote a recent review paper (Reference 7): "Attempts were made to determine the plasma parameters from the electron saturation region.... However, the form of this part of the characteristic is greatly influenced by reflections. These attempts were therefore not continued".

Thus, it appears that the best estimate of electron density can be obtained from a measurement of the probe current at the plasma potential. At this point, the dominance of the electron current over the ion current is generally sufficient to ensure a reasonably accurate determination of the electron density n_{o-}. Furthermore, there is no problem regarding the determination of the collection area since there is no sheath.

26

IV. PROBE INSTRUMENTATION AND MEASUREMENTS

4.1 Analysis of Double Probes

All probe measurements require that two electrodes be inserted in the plasma and the V-I characteristic measured at their terminals. In electrode discharges, one of these is usually the anode or the cathode, whereas the other is the small Langmuir probe. Since the plasma potential is fixed with respect to the anode (or cathode), there is no problem in setting the probe potential with respect to the plasma to any desired level.

In electrodeless discharges, the problem is slightly different since there is no "built in" potential reference with respect to the plasma. Thus, two probes must be introduced for the measurement, with one probe delivering, and the other collecting, the plasma current. When the areas of both probes are comparable, only a limited portion of the range of currents can be covered. Since one of the probes is always limited to collect no more than the ion saturation current I_{+s}, this range is $-\left| I_{+s} \right| < I < \left| I_{+s} \right|$. Thus, in order to cover the full range of currents which the plasma can deliver, or draw, it is necessary to have one probe considerably larger than the other, so that the ion saturation current it can draw exceeds the electron saturation current delivered by the smaller probe. This arrangement is called a counterprobe arrangement. The schematic diagram of the circuit of a counterprobe and its governing equations are shown in Figure 4.1a. A graphical analysis of this arrangement is carried through in Figures 4.1b, c and d.

27

ANALYSIS OF COUNTERPROBE ARRANGEMENT

$$V = V_2 - V_1$$

$$I_p = I_{p2} = -I_{p1}$$
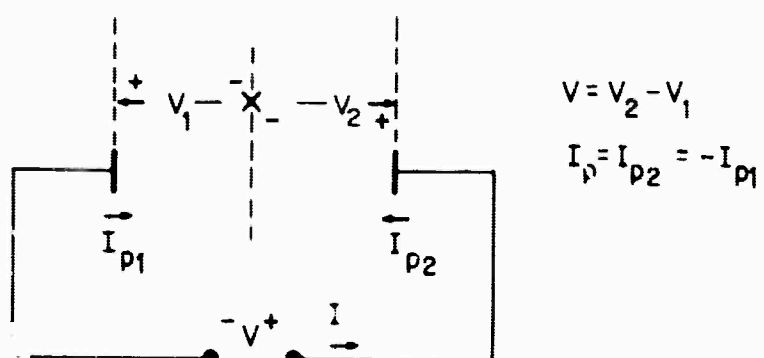
(a) SCHEMATIC DIAGRAM OF COUNTERPROBE ARRANGEMENT
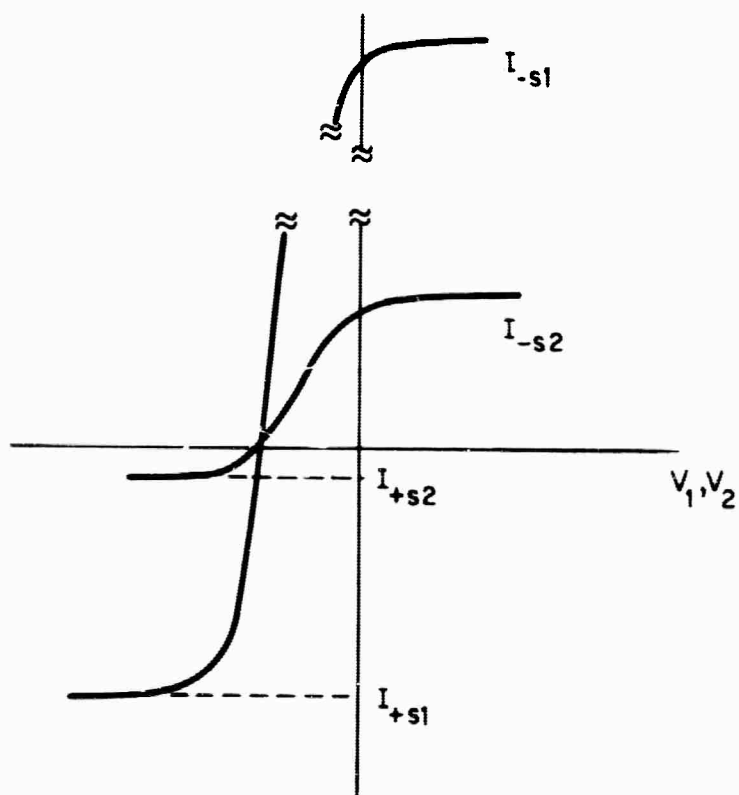
(b) V-I CHARACTERISTIC OF THE TWO PROBES

Figure 4.1 a, b

28

ANALYSIS OF COUNTERPROBE ARRANGEMENT

© GRAPHICAL DETERMINATION OF OPERATING POINT
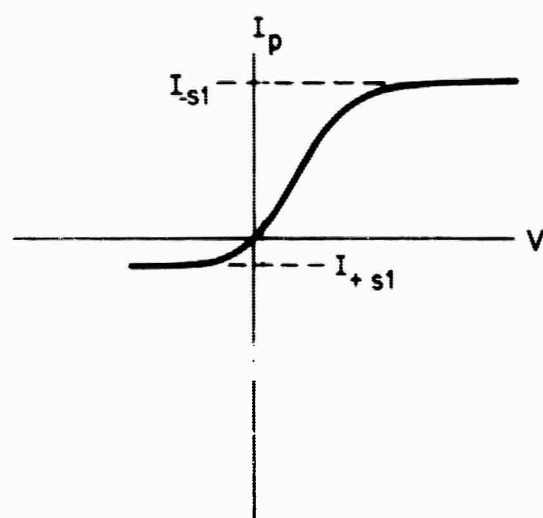
ⓓ V-I CHARACTERISTIC OF DOUBLE PROBE

Figure 4.1 c, d

The individual probe characteristics (with the plasma potential as a reference) are shown in Figure 4.1b. Figure 4.1c indicates the graphical method for solving the circuit equations and determining the cur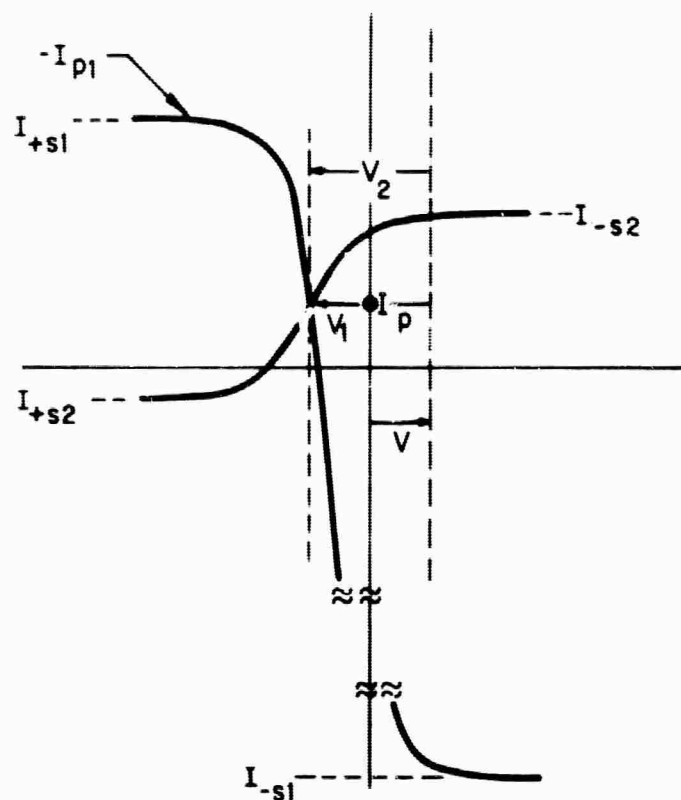rent I corresponding to a given voltage V impressed at the terminals: The characteristic of Probe 2 is inverted with respect to the V – axis, and translated along this axis a distance V corresponding to the impressed voltage. The current is determined at the intersection of the two characteristics.

Some simplicity can be achieved by having the overall V-I characteristic reproduce the shape of the characteristic of the smaller probe. This is accomplished by rendering the slope of the characteristic of the larger probe exceedingly large, by making the area ratio much larger than $(m_+/m_-)^{1/2}$, where m_- is the electron mass. The larger probe then acts effectively as a voltage source, providing the other with a fixed reference V_f with r spect to the plasma potential.

Note that, independent of the area ratio, both probes will float to the same potential V_f with respect to the plasma when the external circuit is open, provided that the characteristics of the plasma surrounding them are the same. Thus, the terminal V-I characteristic of the device always passes through the origin. Any deviation from this condition will indicate a dissimilarity between the plasmas surrounding the two probes. Under these conditions, the voltage required to null the circuit current measures the difference between the floating potentials of the plasmas surrounding each probe.

4.2 Summary

In the following, we summarize the results of the previous discussion, as they apply to the use of a counterprobe in determining the properties of an electrodeless plasma.

30

1. The counterprobe arrangement should duplicate the characteristic of the smaller probe.

2. The electron retardation portion of the curve provides information regarding the shape of the electron distribution function, provided that the latter is isotropic and the probe surface is convex.

$$f(V) \; \alpha \; \frac{d^2 I}{dV^2}$$

3. For a Maxwellian electron distribution, the temperature can be obtained from the logarithmic derivative of the current with respect to the voltage;

$$\frac{1}{I} \quad \frac{dI}{dV} \; = \; - \frac{q}{kT_-}$$

This derivative is constant over the electron retardation region.

The point at which the derivative begins to deviate (drop) from constancy identifies the plasma potential.

4. With T_- known, the electron density n_{o-} can be determined from the probe current at the plasma potential.

5. Ion density may be extracted from the ion saturation portion of the curve. Possible methods are:

(a) Extrapolation of the curve to the plasma potential and use of Equation (3.2.6) (B.B.M. Reference 5);

(b) Use of a point (V, I) on the saturation curve and the K.P. (Reference 7) method. (This requires a guess of the accommodation factor α, but otherwise is straightforward); and

(c) Use of one or two points (V, I) on the saturation curve, and the graphical procedure based on the B.R. analysis. (No guesswork is involved, but the procedure is cumbersone unless the dependence of the probe curves on T_+/T_- is ignored).

6. The ion temperature can be determined with questionable reliability

31

by using the procedure based on the B. R. analysis.

In all measurements based on the use of saturation data, it would be advisable to use several points in order to determine the degree to which the experimental situation conforms to the assumptions of the analysis.

32

V   APPLICATION TO RE-ENTRY VEHICLE EXPERIMENTS

5.1   Experimental Apparatus

The re-entry vehicle associated with the experiment considered here carried an extensive array of Langmuir probes. Some of these were intended to measure the electron temperature and the particle densities of ions and electrons. Others were intended primarily for the measurement of electron density.

Generally, the probes were mounted, in groups of four, on a metallic support structure consisting of a 1/4 to 1/2 inch diameter tube, which projected six to eight inches out of the vehicle skin. (See Figure 5.1 for a sketch). The probes were mounted on insulating cones at various locations along the tubular support structure. The tubular support constituted the ground plane counterprobe for all the probes.

Table 5.1 lists the various probes, their dimensions, their projected distances from the plate, the Debye length expected in the surrounding plasma. The computation of the Debye length was based on information supplied in a series of memos pertaining to the experiment (Reference 13), which contained the anticipated electron densities and expected probe currents (which in most cases were indirectly based on the assumption of a Maxwellian distribution).

5.2   Experimental Data Collection

For data collection a saw-tooth potential having a swing of $\pm$ 10v and a rise rate of 0.4V/msec was applied between each probe and the

33

SKETCH OF PROBE ARRANGEMENT

PROBE

GROUND PLANE
(SUPPORT STRUCTURE)

INSULATOR

PROBES

VEHICLE

34

Figure 5.1
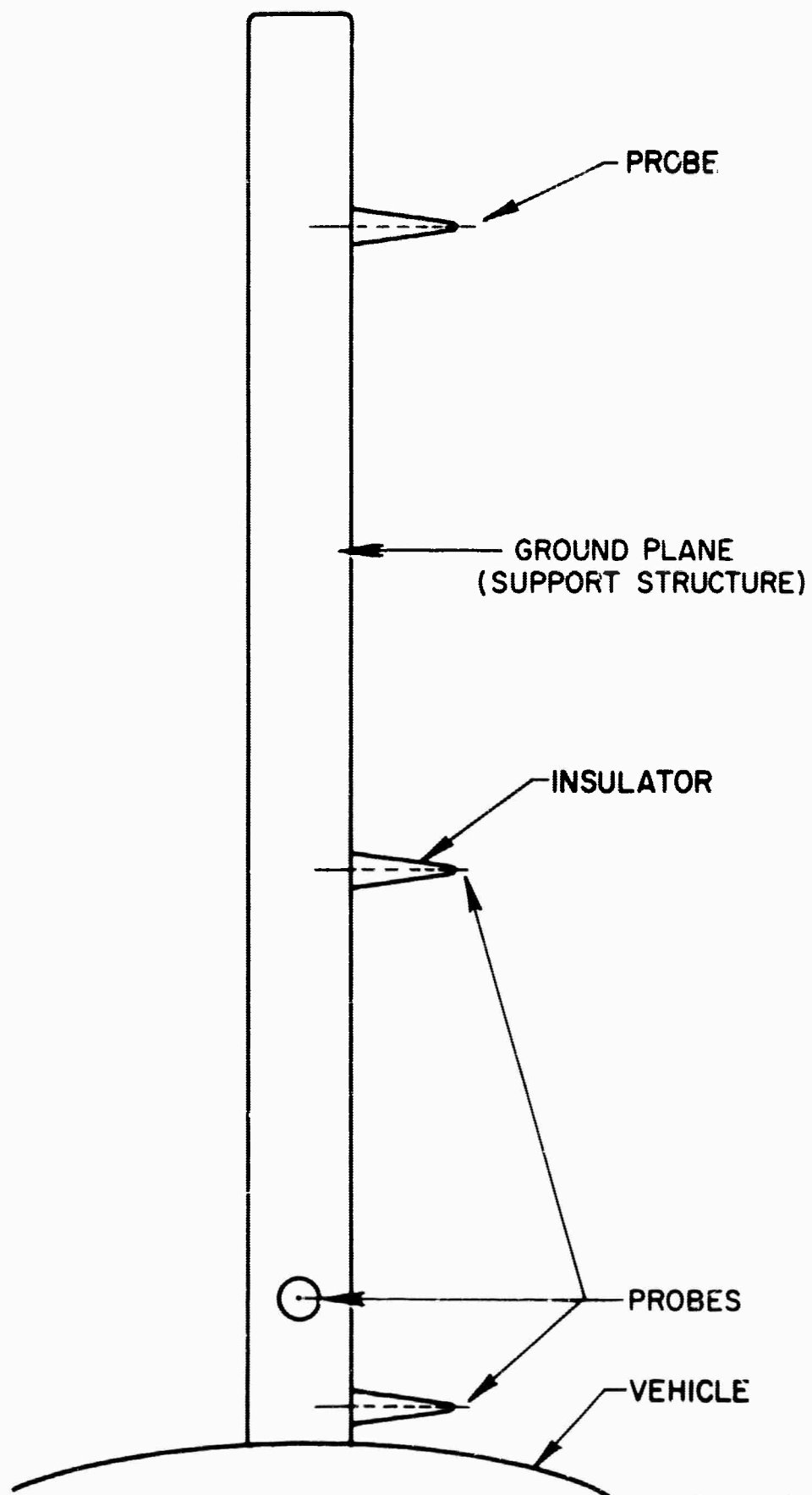
TABLE 5.1   Comparison of the Probe Dimensions with the Debye Length

Probe Location*	Projected Length (inches)	Altitude (kilofeet)	Diameter (mm)	Length (mm)	Debye Length (mm) 5000°K	Debye Length (mm) 14,000°K	Ratio of Characteristic Probe Dimension to Debye Length 5000°K	Ratio of Characteristic Probe Dimension to Debye Length 14,000°K
nose	3,6	300	0.3	0.3	150	250	.001	.0006
131	8	250	0.1	0.1	0.35	0.59	.043	.085
base	1/2, 2, 4, 8	250	0.1	1.0	0.22	0.37	**	**
nose	1/2	300	0.3	0.3	0.19	0.31	.8	.49
nose	1	300	0.3	0.3	0.11	0.19	1.35	.8
208	4	250	0.1	0.1	0.11	0.19	.46	.26
base	1/2, 2, 4, 8	200	0.1	1.0	0.09	0.15	**	**
base	1/2, 2, 4, 8	150	0.1	1.0'	0.049	0.082	**	**
131	4	250	0.1	0.1	0.035	0.058	1.4	.86
131	8	200	0.1	0.1	0.029	0.048	1.7	1.05
166	4	250	.1	.1	.021	.036	2.4	1.4
208	1/2	250	.1	.1	.021	.036	2.4	1.4
base	1/2, 2, 4, 8	100	.1	1.0	.021	.036	**	**
208	4	200	.1	.1	.018	.029	2.8	1.7
166	1/2	250	.1	.1	.016	.026	3.1	1.9
131	1/2	250	.1	.1	.011	.019	4.6	2.6
208	2	200	.1	.1	.008	.013	6.3	3.9
131	8	150	.1	.1	.008	.013	6.3	3.9
166	4	200	.1	.1	.0069	.012	7.3	4.2
166	2	200	.1	.1	.0063	.0105	8	4.8

*Numbers identify Station on Vehicle

** These probes are not amenable to a spherical approx.

TABLE 5.1 (Continued)

Probe Location*	Projected Length (inches)	Altitude (kilofeet)	Diameter (mm)	Length (mm)	Debye Length (mm)		Ratio of Characteristic Probe Dimension to Debye Length	
					$5000^{\circ}K$	$14,000^{\circ}K$	$5000^{\circ}K$	$14,000^{\circ}K$
208	1/4	200	.1	.1	.0055	.009	9.1	5.5
208	1/2	200	.1	.1	.0055	.009	9.1	5.5
166	1/4	200	.1	.1	.0050	.0085	10	6
166	1/2	200	.1	.1	.0050	.0085	10	6
131	4	200	.1	.1	.0048	.0082	11	6
131	1	200	.1	.1	.0035	.0058	14	9
208	4	150	.1	.1	.0035	.0058	14	9
131	1/2	200	.1	.1	.0028	.0046	18	11
208	2	150	.1	.1	.0028	.0046	18	11
208	1/2	150	.1	.1	.0024	.0040	21	13
166	4	150	.1	.1	.0024	.0040	21	13
208	1/4	150	.1	.1	.0022	.0036	23	14
166	2	150	.1	.1	.0022	.0036	23	14
166	1/2	150	.1	.1	.0020	.0033	25	15
166	1/4	150	.1	.1	.0019	.0030	26	17
131	4	150	.1	.1	.0016	.0026	31	19
131	1	150	.1	.1	.0016	.0026	31	19
131	1/2	150	.1	.1	.00105	.0019	48	26

*   Numbers identify
    Station on Vehicle.

support structure (Reference 14). The probe current, $i(t)$, was converted to a voltage, $u(t)$, via a logarithmic amplifier, whose measured transfer function was of the form

$$u = \sum_{k=1}^{m} a_k (\log I)^k \qquad (5.2.1)$$

The following data were transmitted:

(1)   Electron saturation current at the positive end of each swing;

(2)   Ion saturation current at the negative end of each swing;

(3)   The value $(du/dt)_M$ related to the maximum slope of the probe characteristic, and;

(4)   The probe voltage V_M corresponding to the maximum slope.

5.3   Proposed Method of Data Reduction

The proposed method of data reduction (Reference 14) is based on the assumptions that the electron velocity distribution is Maxwellian whereas the ion distribution represents a directed flow. Under these conditions, the break point in the slope of the probe characteristic (which would be identified as a maximum) would indicate the passage of the probe through plasma potential, and provide information regarding the electron temperature. The electron saturation current would be taken as a measure for the electron density, whereas the saturation ion current would give an indication of the quantity $n_{o+}v$, n_{o+} being the ion density and v being the relative velocity between the ions and the probe. In particular, the probe voltage V_M would then be interpreted as the floating potential V_f of the plasma (c.f. Chapter IV regarding the V-I characteristic of a counterprobe).

37

Because the relationship between the logarithm of the probe current I and the monitoring voltage u is not directly linear (c.f. Equation (5.2.1),, it is impossible to infer the temperature T_- directly from the value of $(du/dt)_M$. From Equation 5.2.1

$$\frac{du}{dt} = \sum_{k=1}^{m} k \, a_k \, (\log I)^{k-1} \, \frac{1}{I} \, \frac{dI}{dt} \tag{5.3.1}$$

and, since by assumption

$$I \propto \exp\left(-\frac{qV}{kT_-}\right) \tag{5.3.2}$$

then

$$= \frac{1}{I} \, \frac{dI}{dt} = -\frac{q}{kT_-} \, \frac{dV}{dt} = -0.4 \times 10^3 \frac{q}{kT_-} \, \sec^{-1} \tag{5.3.3}$$

Hence, the relationship,

$$\left(\frac{du}{dt}\right)_m = \sum_{k=1}^{m} k \, a_k \, (\log I_M)^{k-1} \, \left(-0.4 \times 10^3 \, \frac{q}{kT_-}\right) \tag{5.3.4}$$

in which I_M is the probe current when the probe passes through plasma potential, should be used to infer T_-. Since I_M was not measured, the saturation value of the ion current I_{-s} was to be used instead of I_M. Note that, if the voltage u were linear in log I, then Equation (5.3.4) would not involve I_M and would yield T_- directly.

5.4 Evaluation of the Experiment

Without more information regarding the probe characteristic, little can be done by way of data analysis beyond the procedure suggested in the previous section. There are, however, several interesting points raised in connection with the experiment.

38

The first concerns the interpretation of the terminal voltage V_M, when the probe is at plasma potential. It will be recalled that this voltage could be interpreted as the floating potential V_f, provided that the characteristic of the counterprobe arrangement passes through the origin (i.e., $V=0$ when $I=0$). This in turn occurs when the floating potentials of both probes are the same - i.e., when both probes are surrounded by the same ambient plasma.

In some of the situations in this experiment, the tubular structure which served as a "ground plane" was immersed in an inhomogeneous plasma; in fact, the probes mounted on it were intended to measure the inhomogeneity. Thus, if we assume in particular that the temperature is not uniform along the ground plane, each of the small probes (say, the i-th) will be characterized by a particular floating potential V_{fi} with respect to the plasma in its immediate vicinity. The ground plane, however, cannot adjust its potential in this manner, and will therefore float to a potential V_{gi} other than V_{fi} with respect to the plasma surrounding the i-th probe. The potential V_{Mi} measured in the experiment in fact represents $V_{fi} - V_{gi}$.

The second point to be considered is the determination of electron density and temperature, which has to be done simultaneously because of the non-logarithmic nature of the $u - I$ relationship. Under normal circumstances, the temperature determination is considered to be one of the most reliable parts of the experiment, subject of course to the assumption of a Maxwellian electron distribution. This would still be true if the space-potential value I_M of the probe current were employed, rather than the saturation current I_{-s}. The use of I_{-s} introduces a certain error, whose magnitude must be evaluated in terms of the relative significance of the coefficients a_1 and a_0 in the power-series of Equation (5.2.1), as well as in terms of the ratio I_{-s}/I_M.

39

The third point to be considered is the information that can be gathered from the ion saturation measurement. It appears that, for probes located in the stagnation region and also very close to the skin in the boundary layer, one would not be far in error with the assumption of a Maxwellian ion distribution. In fact, consideration of the numbers indicated in the preliminary computation on which the probe and instrumentation design was based (Reference 12) shows a ratio of about 250 between the expected electron saturation current and the ion saturation current, which corresponds to $(m_+/m_-)^{1/2}$ where m_+ is the mass of an NO^+ ion, and m_- is the electron mass and indicates an anticipated Maxwellian distribution for both species.

One might therefore expect to be able to apply some of the results outlined above regarding ion saturation (Sections 3.2 and 3.3). However, if conditir ̇s in the stagnation point are taken as an example, one expects a temperature $(T_+ \approx T_-)$ of about $14,000^\circ K$, or $1.21V$, for the square root of the mass ratio, $(m_+/m_-)^{1/2}$. The floating potential can be estimated as (c.f. Reference 1)

$$V_f = \frac{kT_-}{2q} \log \frac{m_+}{m_-} = -6.6 \text{ volts}$$

Thus, in the course of the $\pm 10^V$ swing of the voltage applied to the counterprobe, the small probe is expected to travel between about $+3.4v$ and $-16.6v$ with respect to the plasma. Thus, the probe goes very deeply into ion saturation. In fact, the ion saturation current is measured when

$$X_p = \frac{qV}{kT_-} \approx \frac{16.6}{1.21} = 13.7$$

If we now refer to the potential profiles shown in Figure 3.5 a, we find that the line $X = 13.7$ lies beyond the "particle trapping limit" out to

40

a ξ of about 14. Thus, one expects those probes whose radii are less than 14 times larger than the local Debye length to operate in the regime where the possibility of particle trapping exists. This covers the probes located in the stagnation region, as a reference to the probe chart shown in Table 5.1 indicates.

The calculation may be repeated for an assumed temperature of 5800°K or about 0.5v, where the floating potential is about -2.75v. Here the ion saturation current would be read when the probe is at about -12.75v with respect to the plasma. Hence χ is about 25.5 and we are operating very deeply in the particle trapping regime. Unfortunately, the computations leading to Figure 3.5 did not cover a sufficiently wider range to indicate the lower bound on probe radius required to avoid the particle trapping regime.

VI   CONCLUSIONS AND RECOMMENDATIONS

6.1   The Re-Entry Experiment

In regards to the experiment discussed in Chapter V, the following conclusions may be drawn:

(1)   The quantity V_M, which is the measured applied voltage when the probe passes through plasma potential, does not represent the floating potential of that probe, in re-entry situations where the ground plane spans a non-isothermal plasma (c.f. Section 5.4).

(2)   In the determination of both the electron density n_{o-} and the electron temperature T_-, the measured electron saturation current has been employed rather than the electron current at plasma potential. Therefore, the calculated values of both n_{o-} and T_- are incorrect, since they include the effects of reflected electrons (c.f. Sections 2.2, 3.3 and 5.4).

(3)   Based on the estimated values of densities and temperatures (Reference 13), calculations indicate that many probes operate within the region where particle trapping may occur (c.f. Sections 3.2 and 5.4). The magnitude of the potential error introduced by particle trapping cannot yet be successfully calculated using existing theoretical models.

(4)   In order to determine the regime of operation, the complete probe curve is necessary. Since only three points were telemetered, this curve cannot be constructed. Therefore, a suitable data reduction procedure cannot be selected.

6.2 The General Usefulness of Probe Measurements

In view of the information presented in Chapters II – IV, the following conclusions may be drawn regarding the determination of the density and temperatures of ions and electrons by means of a Langmuir probe.

(1)   The electron distribution in energy can be determined from probe data in the electron retardation regime. If the distribution is Maxwellian, the electron temperature can be determined from the constant logarithmic derivative of the probe current with respect to probe voltage. The probe is at plasma potential when the logarithmic derivative begins to deviate from constancy.

(2)   The electron density is best determined from the probe current at plasma potential.

(3)   The ion density can be determined from the ion saturation portion of the probe curve, either directly (K. P. method or B. R. method) or after extrapolation to plasma potential (B. B. M.). Care should be exercised to avoid the possible occurrence of particle trapping.

(4)   The ion temperature may be determined from the ion saturation portion of the curve with questionable reliability, since the ion current varies only by 20% over the range

$$ c < \frac{T_+}{T_-} < 1 $$

6.3 Recommendations for Future Experimental Work

In view of what was said above, it appears that it would be advisable, and in some cases necessary, to obtain the full probe curve. This is necessary in order to:

43

(1)   Obtain more information regarding the electron distribution, or at least verify that it is Maxwellian;

(2)   Determine the nature of the phenomena that dominate the saturation regimes; and

(3)   Extrapolate to plasma potential wherever necessary.

When the full probe curve cannot be obtained, then, in particular, measurements of (1) the electron current at the plasma potential, (2) the external voltage when the probe draws no current, and (3) the logarithmic derivative at some point other than plasma potential in the electron retardation region should be made in addition to the present measurements.

6. 4   Recommendations for Future Theoretical Work

The above discussion indicates that, in sufficiently dilute plasmas, the probe saturation currents may be strongly affected by the presence of trapped particles in the vicinity of the probe. The analysis of probe data in this regime would therefore necessitate a deeper understanding of the effects of such particles. This could be accomplished by means of an extension of the self-consistency techniques described in Section 3. 1 to include effects of _assumed_ distributions of trapped particles.

Furthermore, in order to avoid the trapped particle regime, it may be necessary to employ probe sizes which are large enough to cause the thickness of the sheath to exceed a collision mean free path. A possible approach to the treatment of this situation would consist of modifying the analyses described in Chapter III, to account for an outer, collision-dominated regime to the transition region shown in Figure 3. 1.

44

REFERENCES

1. Loeb, L.B., Basic Processes of Gaseous Electronics (Book), U. of California Press, Berkeley and Los Angeles (1955).

2. Druyvestein, M., Zs. Phys. 64, 781 (1930).

3. Langmuir, I., Phys. Rev. 33, 976 (1929).

4. Allis, W.P., Notes on Plasma Dynamics, M.I.T. Notes. Summer Session 1959.

5. Guthrie, A., and Wakerling, R.K., editors, The Characteristics of Gaseous Discharges in Magnetic Fields (Book), Ch. II, McGraw Hill Book Co., New York (1949).

6. Kagan, Yu. M., and Perel, V.I., Trans. of J.T.P. 7, 1093 (1963).

7. Kagan, Yu. M., and Perel, V.I., Trans. of Soviet Physics Uspekhi 6, 767 (1964).

8. Bernstein, J., and Rabinowitz, J., Phys. Fluids 2, 112 (1959).

9. Allen, J.E., Boyd, R.L.F., and Reynolds, P., Proc. Phys. Soc. 70, 297 (1957).

10. Langmuir, I., and Blodgett, K.B., Phys. Rev. 22, 317 (1923).

11. Langmuir, I., and Blodgett, K.B., Phys. Rev. 24, 49 (1924).

12. Muntz, E.P., Harris, C.J., and Kaegi, E.M., Techniques for Experimental Investigation of the Properties of Electrically Conducting, Hypersonic Flow-Fields, Gen. Electric Technical Information Series, Report #R63 SD27, March 1963.

13. Langmuir Probe Experiments on Re-entry Vehicles, General Electric, Missile and Space Vehicle Division, Program Information Request Release No. 263, from Gurdin Sarap to Dr. T. Riethof, September 17, 1962.

14. Calibration Procedure and Data for Langmuir Probe Instrumentation, AFCRL Report, Contract #AF04(694)-295, March 1962, Prepa   by the Geophysics Corporation of America.